Challenging Glass 6 - Conference on Architectural and Structural Applications of Glass
Louter, Bos, Belis, Veer, Nijsse (Eds.), Delft University of Technology, May 2018.

ISBN 978-94-6366-044-0, https://doi.org/10.7480/cgc.6.2151

Alternative Approaches for the Numerical Simulation of Glass Structural Beams Reinforced with GFRP Laminates

Jorge Rocha, Eduardo Pereira, José Sena-Cruz
ISISE, Minho University, Portugal, e-mail a61858@alunos.uminho.pt

This paper discusses alternative numerical approaches to the analysis of the structural behaviour of glass beams reinforced with GFRP laminates adhesively bonded, which were calibrated and validated from four-point bending tests available in the literature. For this purpose, smeared crack and damaged plasticity models were used to simulate the non-linear behaviour of glass, available in FEMIX and ABAQUS finite element softwares. The interaction between the materials in the composite beams, using polyurethane or epoxy adhesives, was defined thought different strategies. In all cases it was possible to simulate well the non-linear behaviour of glass-GFRP composite beams. However, while the FEMIX (smeared crack model) results showed greater resemblance to the experimental ones, ABAQUS models, showed to be able to capture in greater detail the effects of cracking in theses structural responses.

Keywords: Reinforced Glass Beams, Numerical Analysis, Material Constitutive Models, Non-Linear Behaviour

1. Introduction

Currently, the structural glass has a great relevance in contemporary architecture due to its aesthetic features (Correia et al. 2011; Valarinho et al. 2013). However, the structural behaviour of glass is substantially different from other building materials used, such as the steel and the reinforced concrete (Balan and Achintha 2016). The brittle behaviour of glass and the difficulties in predicting its failure require the adoption of suitable safety measures. In recent years, several reinforcing strategies have been developed to overcome glass brittleness (Martens et al. 2015), particularly the hybrid glass systems with timber (Cruz and Pequeno 2008), steel (Belis et al. 2009; Louter et al. 2012; Louter et al. 2014), Carbon Fiber Reinforcement Polymers, CFRP (Palumbo et al. 2005) and Glass Fiber Reinforcement Polymers, GFRP (Neto et al. 2015; Valarinho et al. 2017; Achintha and Balan 2017; Correia et al. 2011; Valarinho et al. 2013).

As shown in previous studies, the major challenges of numerical simulations in this field are (i) the calibration of the mechanical constitutive models used for glass simulation (namely the parameters that define the non-linear behaviour), (ii) the realistic definition of the structural interaction between materials and (iii) the assessment of the post-cracking behaviour (Valarinho et al. 2017; Bedon and Louter 2014).

The numerical simulations are essential to investigate the structural behaviour of hybrid glass systems. However, the brittle behaviour represents a great difficulty to the numerical simulations of glass, as well as the calibration of the material constitutive models adopted. Several approaches have been used to study critical aspects related to glass structural elements such as (i) the type of interlayer representation and factors that influence its stiffness (temperature and load duration), (ii) the type of interaction between materials (glass and reinforcement) and (iii) the type of constitutive models used to described the non-linear behaviour of the glass and interlayer, as well as the behaviour of the reinforcement.

Different constitutive models suitable for representing brittle or quasi-brittle behaviour of concrete, glass and masonry have been used to simulate the non-linear behaviour of glass. While Neto et al. (2015) used a Discrete Crack Model (DCM), Valarinho et al. (2017), Louter et al. (2010), Bedon and Louter (2016b), Bedon and Louter (2017) and Bedon and Louter (2014) have used Smeared Crack Models (SCM). A Damaged Plasticity Model (DPM) was also used by Bedon and Louter (2016a). The numerical simulations of Bedon and Louter (2016b), Bedon and Louter (2017) and Bedon and Louter (2014) were performed in the ABAQUS finite element software, using the Rankine failure criterion for cracks detection. The “brittle failure” option was adopted to model cracking evolution in Bedon and Louter (2014), the “brittle shear” option was adopted in Bedon and Louter (2017) and Bedon and Louter (2016b). Finally, the study performed in Bedon and Louter (2016a) included the numerical simulation of post-tensioned glass beams using ABAQUS, by means of the “concrete damaged plasticity” model, commonly used for modelling concrete.

This work presents a numerical study of the structural behaviour of glass beams reinforced with GFRP laminates, using Smeared Crack (SCM) and Damaged Plasticity (DPM) models, which are available in FEMIX (Sena-Cruz et al. 2007) and ABAQUS 6.14 (Simula 2012). In order to evaluate the efficiency of these models with regard to the accuracy of the simulation of the post-cracking behaviour, the different numerical responses were analysed and

compared considering the following factors: initial stiffness, cracking load, post-cracking stiffness, crack pattern and progressive failure. For this propose, the material parameters derived by Valarinho et al. (2017), defined based on experimental results of glass-GFRP composite beams tested by Valarinho et al. (2013), were used. These beams were reinforced with GFRP laminates adhesively bonded to the tensile (bottom) face of the glass panel, and then subjected to four-point bending tests.

2. Previous Experimental Programme

The numerical simulations of glass-GFRP composite beams of Valarinho et al. (2017) were based on an exploratory experimental study using four-point bending tests performed at Instituto Superior Técnico (IST) in Lisbon and the results published by Neto et al. (2015), Correia et al. (2011) and Valarinho et al. (2013).

The glass-GFRP composite beam specimens, as shown in Fig. 1, consisted of annealed glass panels, with cross section of 12 × 100 mm^2, reinforced at the bottom face with a GFRP pultruded profile (cross section of 12 × 8 mm^2). These materials were joined through two different adhesives, with a layer of 2.0 mm: (i) a polyurethane adhesive, Sikaflex 265, with low Young's modulus (flexible adhesive), and (ii) an epoxy adhesive, SikaDur 31-fc, with high Young's modulus (stiff adhesive). Their properties are described in a subsequent section.

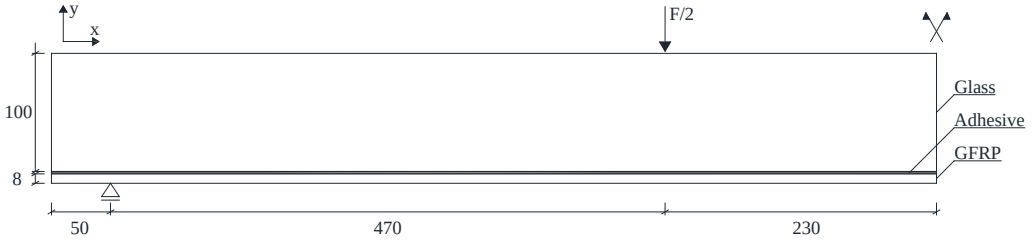

Fig. 1 Schematic representation of the four-point bending test setup. Note: units in [mm].

3. Numerical Simulations

The numerical simulations carried out are based on the material parameters derived by Valarinho et al. (2017). These parameters were obtained from the experimental programme carried out to describe the structural behaviour of the glass-GFRP composite beams made with polyurethane (S*Flex*) and epoxy (S*Dur*) adhesives. Different approaches were used with FEMIX and ABAQUS software, as detailed in the following sections.

3.1. Smeared Crack Model (SCM) - FEMIX

This Section presents the assumptions adopted in the numerical simulation of the glass, GFRP and adhesives for the simulation of the beams with the FEMIX software. Three different strategies were considered to simulate the adhesive joint of composite beams: (i) the *Perfect Bond (PB)* between the glass and GFRP laminate, neglecting the physical existence of the adhesive; (ii) the *Linear Elastic Behaviour (LEB)* of the adhesive, using plane stress (2D models) or solid (3D models) elements, and perfect bond at the GFRP/adhesive and adhesive/glass interfaces; and (iii) the *Non-Linear Behaviour (NLB)* of the joint, using interface elements, simulating the non-linear behaviour of the interfaces (GFRP/adhesive and adhesive/glass) and the adhesive itself.

3.1.1. Annealed Glass

According to the Guideline for European Structural Design of Glass Components (Feldmann and Kasper 2014), in the simulation of the linear elastic behaviour of the annealed glass a Young's modulus, E_g, of 70 GPa, a Poisson's ratio, ν_g, of 0.23 and a tensile strength, $f_{g,t}$, of 30 to 80 MPa were adopted. The glass was simulated assuming linear elastic behaviour in compression and, before cracking, in tension. After cracking, the non-linear behaviour of glass was simulated using a smeared crack model.

After a parametric study, in which the experimental and the numerical results were compared in terms of initial stiffness, cracking load, post-cracking stiffness, crack pattern and progressive failure of the composite beams, Valarinho et al. (2017) defined the glass non-linear features required in this mechanical constitutive model. The following properties were adopted: (i) tensile strength of 50 MPa, (ii) tension-softening diagram with linear shape, (iii) quadratic shear retention factor law, (iv) minimum mode-I fracture energy, G_g, to avoid snap-back instabilities, and (v) crack band width equal to the square root of the finite elements area. A threshold angle of 30º was also defined for the development of new cracks with respect to existing ones, and a maximum number of two cracks in each element was allowed.

3.1.2. GFRP

The GFRP was modelled as a linear elastic material, for both compression and tension, assuming the following mechanical properties: Young's modulus, E_{GFRP}, of 28.7 MPa, Poisson's ratio, ν_{GFRP}, of 0.28.

3.1.3. Interfaces

Based on the parametric study performed by Valarinho et al. (2017), in which the three strategies for the numerical modelling of the adhesive bonded joints were tested, the *PB* conditions were adopted to simulate the composite beam with epoxy adhesive (stiff adhesive).

The *NLB* conditions were adopted for the case of the S*Flex* beam simulation, through a non-linear bond-slip relationship, as suggested by Valarinho et al. (2017). Assuming a bi-linear bond-slip relationship, Table 1 shows the adopted properties: (i) the linear elastic tangential stiffness, K_t, (ii) the shear strength, τ_m, and (iii) the mode-II facture energy, G_m. The linear elastic tangential stiffness is the same in both directions of the adhesive layer. Finally, a high value of the linear elastic normal stiffness, K_n, was adopted for sake of simplicity, as in Valarinho et al. (2017).

Table 1: Mechanical properties used in the simulation of the interface.

	K_n [MPa/mm]	K_t [MPa/mm]	τ_m [MPa]	G_m [N/mm]
S*Flex* beams	10^6	0.4048	1.70	3.50

3.1.4. Mesh Strategy

Taking into account the real geometry and the symmetry conditions of the glass-GFRP composite beams (see Fig. 1), only half span was numerically simulated (l = 700 mm). In the S*Dur* beams, 8-node plane stress elements, with 2 × 2 Gauss-Legendre integration scheme, were used to simulate the glass panel and GFRP laminate (2D models). However, for comparison purposes (reasons are given in Section 3.2.3), 20-node solid elements were also used to simulate the different structural materials (GFRP laminate and glass panel) of the S*Flex* beams (3D models).

In the *NLB* strategy, in agreement with its assumptions, the adhesive layer was simulated by 16-node interface elements with 3 (height) × 2 (thickness) Gauss-Lobatto integration rule. The thickness of the adhesive joint was reproduced positioning the glass panel at a distance of 2 mm from the GFRP laminate, which then filled by the interface elements.

Based on the sensitivity of mesh analysis carried out by Valarinho et al. (2017), elements of 10 × 10 mm^2 provide sufficiently accurate simulations. In the 3D models, only one layer of finite elements was used to describe the beam thickness (10 (width) × 10 (height) × 12 (thickness) mm^3).

3.2. Smeared Crack Model (SCM) – ABAQUS

The assumptions and mechanical properties adopted in the models developed with the FEMIX software (previous Section) were also used in the present case. The GFRP laminate was modelled as a linear elastic material, according to the mechanical properties presented in 3.1.2. In the case of the simulation of the annealed glass, the smeared crack model available in ABAQUS/Explicit is suitable for quasi-static and dynamic analyses (Simula 2012). The computational effort required by ABAQUS/Explicit depends on the density (Simula 2012). A density of 2500 and 1600 kg/m^3 was adopted for the annealed glass and GFRP, respectively.

3.2.1. Annealed Glass

The compressive behaviour of annealed glass was assumed as linear elastic. The brittle failure in tension was properly taken into account through of the "Brittle Cracking" mechanical model, using the "Brittle Shear" option to model crack evolution. This constitutive model is suitable for concrete brittle and quasi-brittle materials, e.g. glass (Bedon and Louter 2016b; Bedon and Louter 2017; Bedon and Louter 2014). Before the material reaches the tensile strength, the linear elastic behaviour was assumed.

In the "Brittle Cracking" model, a Rankine failure criterion is used for the crack detection. The main parameters of this material model are: (i) the tensile strength, (ii) the mode-I facture energy, and (iii) shear retention factor law (in "Brittle Shear" option). Similarly to the FEMIX models (see Section 3.1.1), the following properties were adopted: tensile strength, $f_{t,g}$, of 50 MPa, minimum mode-I facture energy, G_g, quadratic shear retention law and crack band width, h, equal to the square root of the finite elements area. By default, the ABAQUS software assumes a linear tension-softening diagram when the "GFI" option (facture energy cracking criterion) is selected (Simula 2012). Therefore, the maximum crack opening strain, e^{ck}_{max}, required by the "Brittle Shear" option to define the quadratic shear retention law is given by Eq. (1), and was set to 8.0×10^{-4}.

$$e_{\max}^{ck} = \frac{2G_g}{hf_{t,g}} \tag{1}$$

3.2.2. Interfaces

The *PB* and *NLB* strategies were used to simulate the S*Dur* and S*Flex* beams, respectively. The interface GFRP/glass was modelled by "Surface-Based Cohesive Behaviour" with "Progressive Damage and Failure". As this interface model is suitable for situations where the interface thickness is negligible (Simula 2012), the thickness of the adhesive layer was not considered in the simulations.

The constitutive model of the interface was described by the linear elastic normal stiffness, K_n, the linear elastic tangential stiffness in each direction of the adhesive layer, K_t, the normal strength, σ_m, the shear strength, τ_m, and the mode-II facture energy, G_m, assuming a linear softening law. The interface material models used in FEMIX and ABAQUS requires similar parameters and these parameters are defined in Table 1.

3.2.3. Mesh Strategy

Like in FEMIX, with ABAQUS software only half span of the composite beams was numerically simulated. Considering the interface model adopted, the ABAQUS/Explicit does not allow the edge-to-edge contact. Thus, 3D simulation of the S*Flex* beam was performed. The models of S*Dur* and S*Flex* beams were carried out using 4-node plane stress elements (CPS4R) and 8-node solid elements (C3D8R), respectively, both with reduced integration. The adhesive layer was simulated by 4-node zero thickness surface elements (SFM3D4), with 4 integration points (surface-to-surface).

A finite element mesh of 10×10 mm^2 was adopted in the 2D models (S*Dur* beams). In order to ensure symmetry of boundary conditions, two layers of finite elements were used to describe the thickness ($10 \times 10 \times 6$ mm^3) of the S*Flex* beams (3D). Thus, the z-direction displacements of nodes located at the middle-thickness (common to the two layers of finite elements that describe the thickness of the beam) were restrained.

According Chen et al. (2015), (i) the loading scheme, (ii) the loading time, (iii) the damping ratio, (iv) the time increment size and (v) the time integration method are factors that affect the accuracy of quasi-static simulations using models that are intrinsically dynamic. The correct combination of these factors allows to reduce the dynamic effects of the models and obtain quasi-static responses. In ABAQUS, the viscous damping is defined as Rayleigh Damping, where the viscous damping matrix, *C*, is expressed as a linear combination of the mass matrix, *M*, and the stiffness matrix, *K* (see Eq. (2)). The damping ratio for the jth mode of the system can be expressed by expression (3).

$$C = \alpha_0 M + \beta_0 K \tag{2}$$

$$\varsigma_j = \frac{\alpha_0}{2\omega_j} + \frac{\beta_0 \omega_j}{2} \tag{3}$$

The α_0 and β_0 parameters of the Eq. (2) and (3) are proportionality constants for mass and stiffness-proportional damping, respectively. On the other hand, ω_j is the circular frequency corresponding to the jth mode. In the case of *PB* strategy (S*Dur* beams), the period T_1 of the fundamental vibration mode is equal to 0.288 seconds and, consequently, ω_1 has a value of 21.77 rad/s. According to Chen et al. (2015), the loading time should be in the range of $50T_1$ to $100T_1$ (14 to 28 seconds, approximately), with a linear loading scheme and a suitable damping ratio. The time integration method and an automatic time increment size are inherent to the ABAQUS/Explicit. Considering the numerical models performed by Chen et al. (2015), the mass-proportional damping may become unstable. However, mass-proportional damping, which requires less computational effort and, in addition, has a higher damping efficiency for the low frequency vibration modes, was applied in this work.

3.3. Damaged Plasticity Model (DPM) - ABAQUS

The assumptions and mechanical properties adopted in the previous models (see Section 3.2) were also used in the case of the simulations with the Damaged Plasticity Model (DPM), mainly: (i) the GFRP was modelled as a linear elastic material (mechanical properties presented in Section 3.1.2); (ii) the *PB* and *NLB* strategies were used in S*Dur* and S*Flex* beams, respectively; (iii) the "Surface-Based Cohesive Behaviour" with "Progressive Damage and Failure" were used to describe the interface GFRP/glass (mechanical properties presented in Table 1); and (iv) the finite elements CPS4R, C3D8R and SFM3D4 were used to simulate the S*Dur* and S*Flex* beams. Although the DPM is available in ABAQUS/Standard, the simulations were performed in ABAQUS/Explicit to avoid snap-back instabilities, mainly in the simulation of the S*Flex* beams that, comparing with S*Dur* beams, show a more brittle behaviour.

3.3.1. Annealed Glass

As stated before, the glass was modelled with the "Concrete Damage Plasticity" model. This model was originally used in the simulation of reinforced concrete elements (Tao and Chen 2015; López-Almansa et al. 2014; Coronado and Lopez 2006), and then extended to the simulation of other quasi-brittle materials, e.g., glass (Bedon and Louter 2016a) and masonry.

The mechanical parameters required to simulate the tensile behaviour of glass are: (i) the yield stress, σ_t, (ii) the mode-I facture energy, G_f, and (iii) the damage law, defined by the d_t parameter (Simula 2012). The minimum mode-I facture energy was adopted to avoid snap-back instabilities, such as in the case of the smeared crack models (see Sections 3.1 and 3.2). As mentioned in 3.2.1, when the GFI option is selected, the ABAQUS software assumes a linear tension-softening diagram. Therefore, the maximum total displacement, u_t, which also includes the elastic deformation, was determined multiplying the Eq. (4) and its value is equal to 1.514×10^{-2} mm.

Since glass has a brittle nature, the plastic strain, u_t^{pl}, is null ($u_t^{el} = u_t$). According to Simula (2012), an excessive damage factor may have a critical effect on the rate of convergence. A damage factor of 0.99 was assigned to the maximum total displacement, which corresponds to 99 % reduction of the stiffness, taking into account Simula (2012) recommendations. Based in this aspects, the damage law adopted is presented in Fig. 2, as well as the corresponding mechanical constitutive model.

$$u_{\max} = \frac{hf_{t,g}}{E_g} + \frac{2G_g}{f_{t,g}} \tag{4}$$

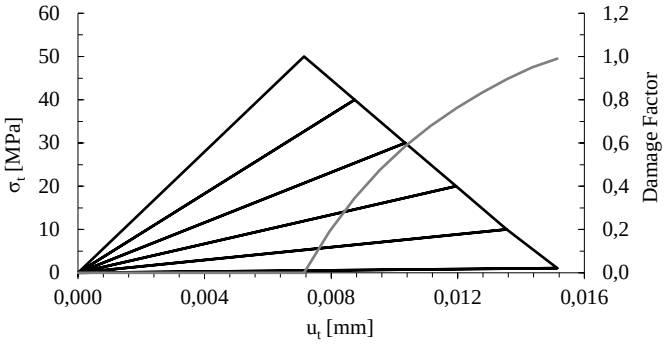

Fig. 2 Damaged law adopted for simulating glass behaviour.

4. Results and Discussion

Fig. 3, 4 and 5 show the load *vs.* vertical displacement diagrams of S*Dur* and S*Flex* beams obtained from three material models, as well as the crack pattern at relevant phases: (i) beginning and end of the post-cracking stage of S*Dur* beams, and (ii) after the cracking for the S*Flex* beams. In S*Dur* beams, the crack pattern is also presented at the middle of the post-cracking stage to evaluate the evolution of cracking. The load (F) is presented as a function of the vertical displacement at middle-span (u). The SCM and DPM models included in ABAQUS do not provide the crack pattern visualisation. So, it was decided to present the strains fields in the x-direction (LE11 according to software terminology).

The S*Dur* beams analysis was stopped when the cracking load was recovered. On the other hand, in the simulation of S*Flex* beams, the analysis was stopped when the vertical displacement of 14 mm was attained, since its post-cracking stages showed a monotonic increase of stress and a steady behaviour, besides the models present many instabilities, making the computations very difficult from this displacement onwards.

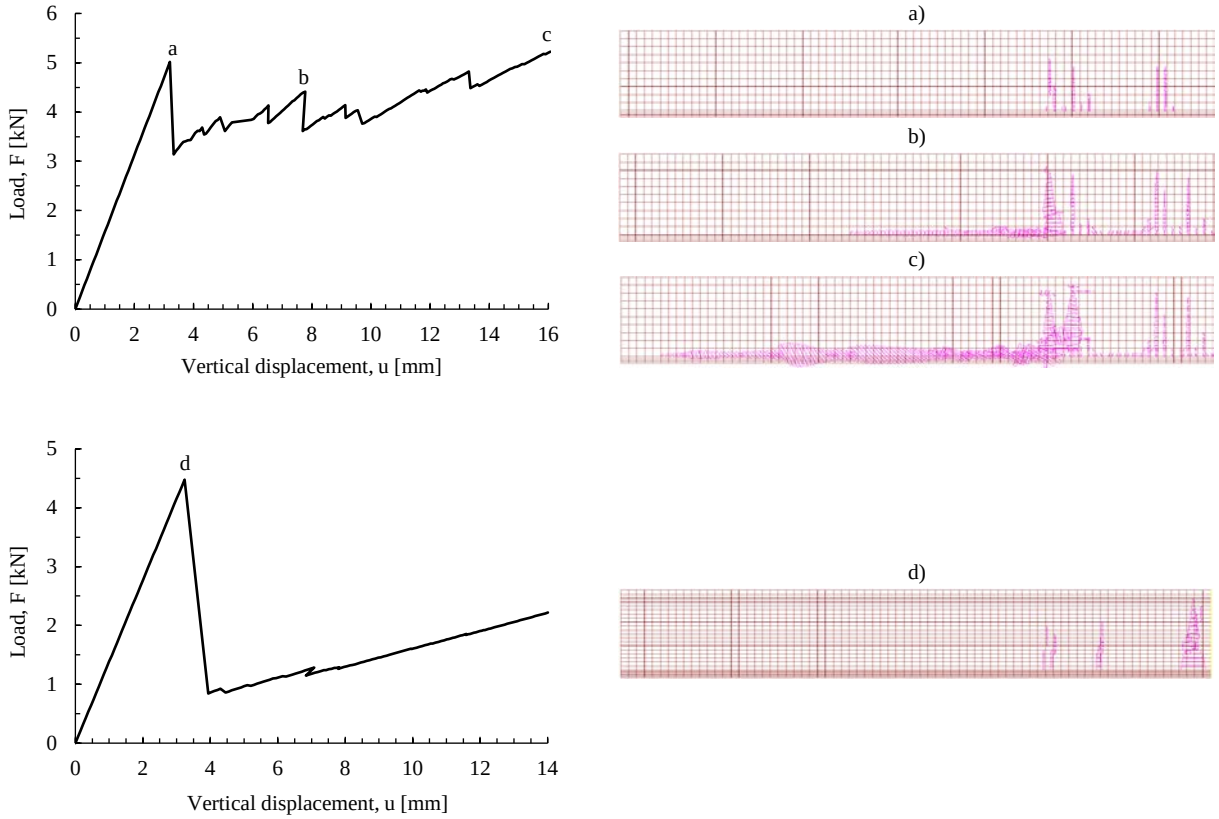

Fig. 3 Load *vs*. vertical displacement diagrams of the S*Dur* (top left side) and S*Flex* (bottom left side) beams, obtained from the FEMIX using a smeared crack model, as well as the crack pattern a), b), c) and d) at different phases (right side).

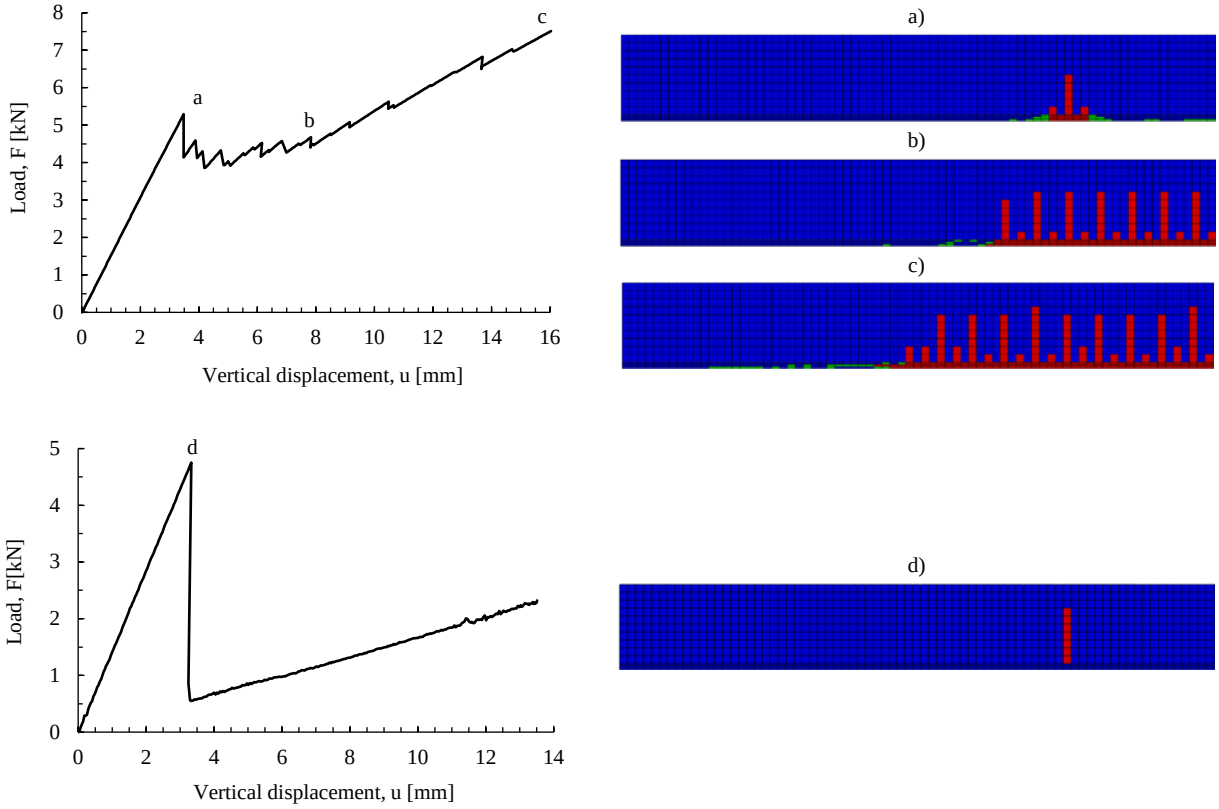

Fig. 4 Load vs. vertical displacement diagrams of the S*Dur* (top left side) and S*Flex* (bottom left side) beams, obtained from the ABAQUS using a smeared crack model, as well as the crack pattern a), b), c) and d) at different phases (right side).

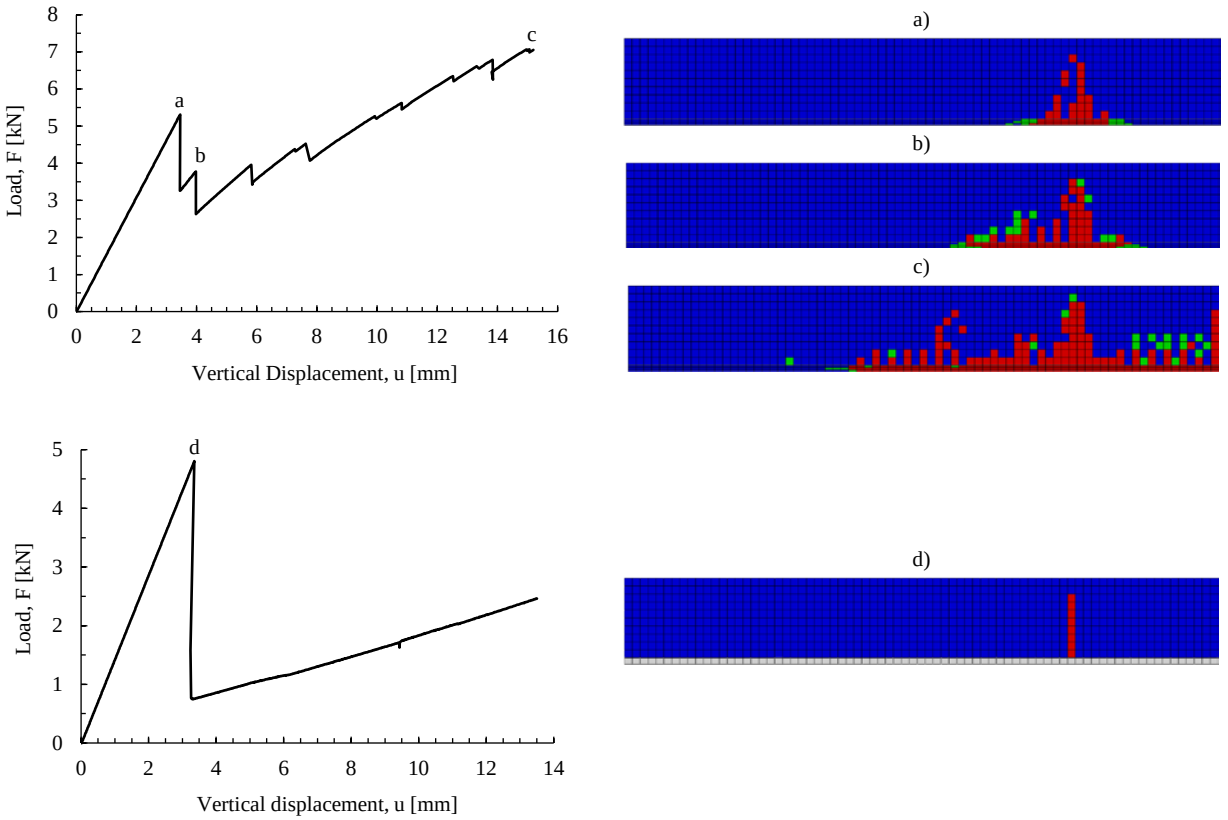

Fig. 5 Load *vs*. vertical displacement diagrams of the S*Dur* (top left side) and S*Flex* (bottom left side) beams, obtained from the ABAQUS using a damaged plasticity model, as well as the crack pattern a), b), c) and d) at different phases (right side).

The load *vs*. vertical displacement diagrams obtained by using distinct models are plotted and compared in the Fig. 6 for the composite beams made with epoxy (S*Dur*) and polyurethane (S*Flex*) adhesives. Table 2 presents, for the simulated beams, the main parameters characterizing its structural behaviour: elastic stiffness, K_{el}, cracking load, F_{ck}, and corresponding vertical displacement, u_{ck}.

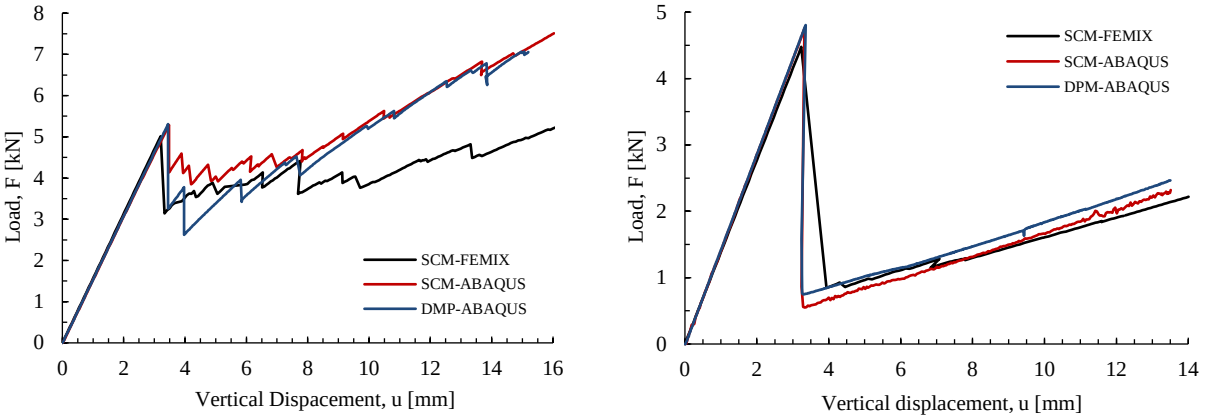

Fig. 6 Load *vs*. displacement diagrams of S*Dur* (left side) and S*Flex* (right side) beams obtained with the distinct models.

Table 2: Elastic properties of the S*Dur* and S*Flex* beams defined from the responses obtained in different models.

	S*Dur* beams			S*Flex* beams		
	K_{el} [kN/mm]	F_{cr} [kN]	u_{ck} [mm]	K_{el} [kN/mm]	F_{cr} [kN]	u_{ck} [mm]
SCM-FEMIX	1.565	5.014	3.203	1.384	4.399	3.179
SCM-ABAQUS	1.527	5.289	3.580	1.424	4.753	3.326
DPM-ABAQUS	1.540	5.312	3.450	1.428	4.813	3.355

4.1. SDur beams

The first crack appears between the loading points in all models, inside the pure bending region. Taking into account this information, for the S*Dur* beams, which were modelled assuming the perfect bond between glass and GFRP (*PB* strategy), the analytical cracking load, F_{ck}, is given by Eq. (5), where $I_y = 1.111 \times 10^6$ mm^4 (homogenized cross section), $y_g = 56.285$ mm, $x_1 = 470$ mm and $h_{gfrp} = 8.0$ mm. On the other hand, considering the elastic integration method and omitting the shear effects, the analytical vertical displacement at middle-span corresponding to the cracking load, u_{ck}, is provided by Eq. (6), where $x_2 = 230$ mm and $EI_y = 7.779 \times 10^{10}$ N·mm^2. Table 3 presents the elastic properties of S*Dur* beams, analytically calculated from Eqs. (5) and (6). The cracking load obtained with the SCM-FEMIX static analysis is slightly greater (2.4 %) when compared to the analytical value. This is because, in the first case, failure occurs only when the integration point, which is slightly above the bottom edge of the glass panel, reaches the tensile strength.

$$F_{ck} = \frac{2 f_{t,g} I_y}{\left(y_g - h_{gfrp}\right) x_1} \tag{5}$$

$$u_{ck} = \frac{1}{EI_y}\left(\frac{F_{ck} x_1}{4} x_2^2 - \frac{F_{ck} x_1 x_2}{2} x_2 + \frac{F_{ck}}{12} x_1^3 - \left(\frac{F_{ck} x_1^2}{4} + \frac{F_{ck} x_1 x_2}{2}\right) x_1\right) \tag{6}$$

Table 3: Mechanical properties of the elastic behaviour of SDur beams analytically calculated.

	K_{el} [kN/mm]	F_{cr} [kN]	u_{ck} [mm]
S*Dur* beams	1.530	4.897	3.201

The ABAQUS models show a higher cracking load, F_{ck}, when compared to SCM-FEMIX, probably due to the different types of mesh used in both cases. While in the FEMIX model 8-node plane stress elements with 4 integration points (2 × 2 Gauss-Legendre integration scheme) were adopted, the ABAQUS/Explicit only supports 4-node reduced integration elements with 1 integration point (CPS4R). The 2 × 2 integration scheme in 4-node elements is not supported by ABAQUS/Explicit, as well as 8-node elements with 3 × 3 integration scheme or 2 × 2, for reduced integration (Simula 2012). Due to this, eventually the finite elements used in SCM-FEMIX may show greater resolution to describe the deformation or stress fields than the finite elements of ABAQUS models.

In SCM-FEMIX (static analysis), the elastic stiffness appears to remain constant during pre-cracking stage. In contrast, the elastic stiffness of SCM-ABAQUS shows a gradual decrease, from the initial 1.548 to 1.488 kN/mm immediately before reaching the peak load. On the other hand, DPM-ABAQUS showed a milder decrease during the elastic stage, from the initial 1.543 kN/mm to 1.539 kN/mm immediately before cracking. The dynamic effects in ABAQUS/Explicit are particularly sensitive to the loading time. When different loading times were adopted using the same model, it was verified that the linearity of the elastic stiffness decreased with the increase of the loading time. However, an excessive reduction of the loading time also increases the dynamic effects. As mentioned in 3.2.3, the loading time was defined considering the indicative value proposed by Chen et al. (2015), $50T_1$ to $100T_1$, and the required computational effort. The loading time of 20 seconds was adopted.

The load shows an increasing trend at the end of the post-cracking stages. The development of new cracks in the ABAQUS models is followed by a greater stiffening effect when comparing to the results obtained with FEMIX, which is probably explained by interpreting the cracking patterns obtained (see Fig. 2, 3 and 5). In ABAQUS models cracking stabilization was reached for a smaller vertical displacement (approximately 8.0 mm). As a consequence, an apparently lower number of total cracks may have led to the greater stiffening effect. At the later part of the post-cracking stage, the stiffening trajectory in all models seems to be approximately similar, probably due to cracking stabilization.

With respect to the crack pattern obtained at failure, the three models show significant differences. The collapse of the glass through the damaging of the bottom edge and subsequent detachment of the GFRP laminate were satisfactorily represented by CSM-FEMIX. At the end of the post-cracking stage, new cracks between the support and the loading point also propagate in the horizontal direction. These cracks, which eventually lead to the laminate detachment, are not clearly visible in the case of ABAQUS models.

4.2. SFlex beams

The SCM and DPM-ABAQUS cracking loads were 6.7 % and 8.0 % larger than SCM-FEMIX, respectively (see Table 2). Two factors can explain this difference: (i) the number of integration points used in each model are distinct and (ii) the absence of the modelling of the adhesive joint in the case of both ABAQUS models.

In SCM and DPM-ABAQUS, 8-node solid elements with 1 integration point, C3D8R, were used. In these models, S*Flex* beams were discretized using two finite elements layers (see Section 3.2.3). However, the increment of integration points occurred in the perpendicular direction (z-direction) to the plane analysed (x-y plane). In contrast, in the case of the SCM-FEMIX, 20-node solid elements with 8 integration points were used, which lead to increased discretization for the representation of the stress fields. As a result, the maximum stress at the mostly stressed fibres in the cross section may be reached for slightly lower loads.

The elastic stiffness obtained, K_{el}, was similar in all models of S*Flex* beams (see Table 2). As in the case of the S*Dur* beams, the dynamic effects of the ABAQUS/Explicit had influence on the load *vs*. vertical displacement numerical responses obtained. The elastic stiffness of SCM-ABAQUS was essentially constant, changing from 1.449 kN/mm at the onset and 1.444 kN/mm right before the peak load was reached. Also in the case of the DPM-ABAQUS an essentially constant elastic stiffness was observed, starting at 1.438 and reaching 1.440 kN/mm right before the peak load. As the S*Flex* beams were associated to the formation of much less cracks than S*Dur* beams, a loading time of 12.5 seconds was sufficient to reduce the dynamic effects on the structural responses for both ABAQUS models.

All three numerical responses obtained are essentially similar when the post-cracking stage is considered. Nevertheless both the ABAQUS models have resulted in the development of one single vertical crack in both cases, while the SCM-FEMIX has shown a final crack pattern with three cracks (see Fig. 2, 3 and 5). The post-cracking load obtained in DPM-ABAQUS is higher than the ones obtained in the other models. This difference can be explained by the residual stress and stiffness in the crack, which is a consequence of the difficulty that plasticity models experience in dealing with strong deformation localization. The DPM does not support an absolute damaged factor of 1.0 at the maximum crack opening displacement, as mentioned in Section 4.1 for the S*Dur* beams. However, the DPM-ABAQUS and the FEMIX models showed similar stiffness in the post-cracking stage, since the resistant mechanism and the mechanical properties of the adhesive layer are the same.

The behaviour of the S*Flex* beams throughout the pre-cracking stage was mostly influenced by the glass panel due to its much greater stiffness. The GFRP laminate has showed low levels of tensile stress before cracking was reached. Therefore the neglecting of the adhesive thickness in the discretization had greater influence at the post-cracking stage.

5. Conclusions

In this paper, an extensive numerical study was carried out in order to assess the performance of the most commonly used constitutive models to simulate the behaviour of glass structural elements, in particular the smeared crack and the damaged plasticity models. For this purpose the experimental results obtained in a previous study, after testing glass beams reinforced with GFRP laminates adhesively bonded, were considered.

The main conclusions may be summarized as follows:

- All mechanical constitutive models used showed to be suitable for conveniently simulating the non-linear behaviour of glass structural beams. The cracking patterns formed and the progressive loss of stiffness observed in the experiments were correctly captured by the numerical models, particularly in the case of the S*Flex* beams which have an extremely brittle behaviour. The different material models adopted have been essentially characterized by a similar set of non-linear parameters: tensile strength, mode-I fracture energy, shape of the tension-softening diagram and type of shear retention factor which, in the case of the Damaged Plasticity Model, was replaced by the damage law;
- When compared to the FEMIX models, the computational effort required by ABAQUS models was very high, especially in the case of the 3D models of S*Flex* beams. The ABAQUS/Explicit can also be used for quasi-static analysis by properly prescribing the loading time, the mass scaling factor, the loading scheme and, especially, the damping ratio. Although the damping ratio reduces the dynamic effects of the structural responses, its influence on the results obtained requires special attention. Usually, considering the brittle nature of glass, the damping ratio is a numerical parameter which is very difficult to calibrate by experimental means;
- SCM-FEMIX provided more accurate results, which were independent of dynamic factors like the loading time and other parameters that are very difficult to validate experimentally, such as the damping ratio;
- The Damaged Plasticity Model is suitable to simulating the non-linear behaviour of glass structural elements. In comparison to Smeared Crack Models (SCM), DPM also showed to be able to capture the post-cracking response of glass-GFRP composite beams. However, this material model only allows a maximum damage factor of 0.99, which causes a reduction of the initial elastic stiffness of 99 %. Therefore, the cracks always retain a residual stress corresponding to 1.0 % of the undamaged state. The effects of residual stress are present in the post-cracking load of S*Flex* beams, which only developed a single crack. The finite elements with non-linear behaviour, despite their low stiffness, showed to be able to transfer load between adjacent elements.
- The numerical models performed in ABAQUS/Explicit, of a dynamic nature, showed to be able to capture in greater detail the effects of cracking on the structural responses because, as opposed to FEMIX models, much smaller load steps are easily implemented and these result in better stability and precision during crack formation.

References

Achintha, M., Balan, B.: Characterisation of the mechanical behaviour of annealed glass – GFRP hybrid beams. Constr. Build. Mater. 147, 174–184 (2017)

Balan, B., Achintha, M.: Experimental and Numerical Investigation of Float Glass-GFRP Hybrid Beams. In: Belis, Bos, Louter (eds.) Challeging Glass 5 - Conference on Architectural and Structural Applications of Glass, pp. 281–296. Ghent (2016)

Bedon, C., Louter, C.: Exploratory numerical analysis of SG-laminated reinforced glass beam experiments. Eng. Struct. (2014). doi: 10.1016/j.engstruct.2014.06.022.

Bedon, C., Louter, C., 2016a. Finite-element analysis of post-tensioned SG-laminated glass beams with mechanically anchored tendons. Glas. Struct. Eng. (2016a). doi: 10.1007/s40940-016-0020-7.

Bedon, C., Louter, C.: Finite-Element Numerical Simulation of the Bending Performance of Post-Tensioned Structural Glass Beams with Adhesively Bonded CFRP Tendons. Am. J. Eng. Appl. Sci. 9(3), 680–691 (2016b)

Bedon, C., Louter, C.: Finite Element analysis of post-tensioned SG-laminated glass beams with adhesively bonded steel tendons. Compos. Struct. 167, 238–250 (2017)

Belis, J., Callewaert, D., Delincé, D., Van Impe, R.: Experimental failure investigation of a hybrid glass / steel beam. Eng. Fail. Anal. (2009). doi: 10.1016/j.engfailanal.2008.07.011.

Chen, G.M., Teng, J. G., Chen, J. F., Xiao, Q.G.: Finite element modeling of debonding failures in FRP-strengthened RC beams: A dynamic approach. Comput. Struct. (2015). doi: 10.1016/j.compstruc.2015.05.023

Coronado, C.A., Lopez, M.M.: Sensitivity analysis of reinforced concrete beams strengthened with FRP laminates. Cem. Concr. Compos. 28(1), 102–114 (2006).

Correia, J.R., Valarinho, L., Branco, F.A.: Post-cracking strength and ductility of glass-GFRP composite beams. Compos. Struct. 93(9), 2299–2309 (2011).

Cruz, P.J.S., Pequeno, J.: Timber-Glass Composite Beams: Mechanical Behaviour & Architectural Solutions. Challenging Glass, 439–448 (2008).

Feldmann, M., Kasper, R.: Report EUR 26439 EN - Guidance for European Structural Design of Glass Components. Institute for the Protection and Security of the Citizen, Joint Research Center (eds.). Luxembourg (2014). doi: 10.2788/5523

López-Almansa, F., Alfarah, B., Oller, S.: Numerical simulation of RC frame testing with damaged plasticity model comparison with simplified models. In 2nd European Conference on Earthquake Engineering and Seismology, pp. 1–12. Instabul (2014)

Louter, C., Belis, F., Veer, F., Lebet, J.P.: Structural response of SG-laminated reinforced glass beams; experimental investigations on the effects of glass type, reinforcement percentage and beam size. Eng. Struct. (2012). doi: 10.1016/j.engstruct.2011.12.016

Louter, C., Cupac, J., Lebet, J. P.: Exploratory experimental investigations on post-tensioned structural glass beams. J. Facade Des. Eng. 2, 3–18 (2014)

Louter, C., Graaf, A., Rots, J.: Modeling the Structural Response of Reinforced Glass Beams using an SLA Scheme. In: Bos, Louter, Veer (Eds.) Challenging Glass 2 - Conference on Architectural and Structural Applications of Glass. Delft (2010)

Martens, K., Caspeele, R., Belis, J.: Development of composite glass beams - A review. Eng. Struct. (2015). doi: 10.1016/j.engstruct.2015.07.006.

Neto, P., Alfaiate, L., Valarinho, J. R., Branco, F. A., Vinagre, J.: Glass beams reinforced with GFRP laminates: Experimental tests and numerical modelling using a discrete strong discontinuity approach. Eng. Struct. (2015). doi: 10.1016/j.engstruct.2015.04.002.

Palumbo, M., Palumbo, M., Mazzucchelli, M.: A New Roof for the XIIIth Century 'Loggi de Vicari' (Arquà Petrarca - PD Italy) Based on Structural Glass Trusses: A Case Study. Glass Processing Days. Tempere, Finland (2005)

Sena-Cruz, J., Barros, J., Azevedo, A., Ventura-Gouveia, A.: Numerical Simulation of the Nonlinear Behavior of Rc Beams Strengthened With Nsm Cfrp Strips. In CMNE 2007 - Congress on Numerical Methods in Engineering and XXVIII CILAMCE - Iberian Latin-American Congress on Computational Methods in Engineering, pp. 13–15. Porto (2007)

Simula: ABAQUS computer software and Online Documentation v6.12. Dassault Systèmes Simula Corp (eds.). Providence, USA (2012)

Tao, Y., Chen, J.F.: Concrete Damage Plasticity Model for Modeling FRP-to-Concrete Bond Behavior. Comput. Struct. (2015). doi: 10.1061/%28ASCE%29CC.1943-5614.0000482

G. M. Chen, J. G. Teng, J. F. Chen, and Q. G. Xiao, 'Finite element modeling of debonding failures in FRP-strengthened RC beams : A dynamic approach', Comput. Struct., vol. 158, pp. 167–183, 2015.

Valarinho, L., Sena-Cruz, J., Correia, J. R., Branco, F. A.: Numerical simulation of the fl exural behaviour of composite glass-GFRP beams using smeared crack models. Compos. Part B Eng. 110, 336–350 (2017)

Valarinho, L., Correia, J.R., Branco, F. A.: Experimental study on the flexural behaviour of multi-span transparent glass-GFRP composite beams. Constr. Build. Mater. (2013). doi: 10.1016/j.conbuildmat.2012.11.024.